Brain Connectivity and Behavioral Changes in a Spaceflight Analog Environment with Elevated CO_2

Heather R. McGregor[1], Jessica K. Lee[2], Edwin R. Mulder[2], Yiri E. De Dios[3], Nichole E. Beltran[3], Igor S. Kofman[3], Jacob J. Bloomberg[4], Ajitkumar P. Mulavara[3] & Rachael D. Seidler[1*]

[1] Department of Applied Physiology and Kinesiology, University of Florida, Gainesville, FL;
[2] Institute of Aerospace Medicine, German Aerospace Center, Cologne, Germany;
[3] KBR, Houston, TX;
[4] NASA Johnson Space Center, Houston, TX;

HRM analyzed fMRI data and brain-behavior associations. JKL and YED analyzed behavioral data. JKL collected data. JKL, NEG, ISK set up the experiment. RDS, ERM, JJB, APM designed the experiment and secured funding. HRM drafted the manuscript. HRM, JKL, ERM, JJB, RDS edited the manuscript.

Declarations of interest: None

***Corresponding author:**
Rachael D. Seidler, Ph.D.
University of Florida
1864 Stadium Rd.
Gainesville, FL 32611
Email: rachaelseidler@ufl.edu

Keywords
Bed Rest, Spaceflight, CO_2, Resting-state fMRI, Functional Connectivity, Cognition, Sensorimotor

ABSTRACT

Astronauts are exposed to microgravity and elevated CO_2 levels onboard the International Space Station. Little is known about how microgravity and elevated CO_2 combine to affect the brain and sensorimotor performance during and after spaceflight. Here we examined changes in resting-state functional connectivity (FC) and sensorimotor behavior associated with a spaceflight analog environment. Participants underwent 30 days of strict 6^o head-down tilt bed rest with elevated ambient CO_2 (HDBR+CO_2). Resting-state functional magnetic resonance imaging and sensorimotor assessments were collected 13 and 7 days prior to bed rest, on days 7 and 29 of bed rest, and 0, 5, 12, and 13 days following bed rest. We assessed the time course of FC changes from before, during, to after HDBR+CO_2. We then compared the observed connectivity changes with those of a HDBR control group, which underwent HDBR in standard ambient air. Moreover, we assessed associations between post-HDBR+CO_2 FC changes and alterations in sensorimotor performance. HDBR+CO_2 was associated with significant changes in functional connectivity between vestibular, visual, somatosensory and motor brain areas. Several of these sensory and motor regions showed post-HDBR+CO_2 FC changes that were significantly associated with alterations in sensorimotor performance. We propose that these FC changes reflect multisensory reweighting associated with adaptation to the HDBR+CO_2 microgravity analog environment. This knowledge will further improve HDBR as a model of microgravity exposure and contribute to our knowledge of brain and performance changes during and after spaceflight.

This study was supported by NASA grant #80NSSC17K0021. HRM was supported by a NSERC postdoctoral fellowship and a NASA Human Research Program grant augmentation.

MRI files for this study will be placed in the NASA data repository upon study completion.

INTRODUCTION

Spaceflight elicits sensorimotor adaptive processes due to altered sensory inputs. Upon initial exposure to microgravity, crewmembers typically experience sensorimotor disturbances and disorientation, but they gradually adapt to body unloading, alterations in vestibular, and somatosensory inputs (Paloski et al., 1994, 1992; Reschke et al., 1998), as well as to headward fluid shifts (Lee et al., 2019; Roberts et al., 2017). In addition to microgravity, astronauts must also adapt to the mildly hypercapnic environment of the International Space Station (ISS) where carbon dioxide (CO_2) levels average 0.5% -- approximately ten times higher than typical ambient levels (~0.04%) on Earth (Law et al., 2014). On Earth, exposure to 3% CO_2 over several hours produces headaches while resting. During mild exertion, subjects begin to report headaches at 2% CO_2 (Schlute, 1964). Mild impairments in visuo-motor performance have been reported at levels as low as 1.2% CO_2 (Manzey and Lorenz, 1998). Onboard the ISS, astronauts report CO_2-related symptoms at lower CO_2 levels than would be expected on Earth; astronauts are more prone to headaches (Law et al., 2014) and experience “space fog” characterized by slowed mental abilities and poor concentration (Kanas and Manzey, 2008; Welch et al., 2009). This suggests that microgravity and elevated CO_2 levels may interact to negatively impact crewmember health and mission success.

Astronauts return to Earth in a microgravity-adapted state, exhibiting pronounced impairments in balance (Cohen et al., 2012; Paloski et al., 1994), locomotion (Bloomberg and Mulavara, 2003; Courtine and Pozzo, 2004; McDonald et al., 1996; Mulavara et al., 2018, 2010), and manual motor control (Manzey et al., 2000; Moore et al., 2019). Readaptation to Earth’s 1g environment takes place over the course of days or weeks (Miller et al., 2010; Mulavara et al., 2018, 2010).

Although the behavioral effects of spaceflight have been well-documented, the neural mechanisms underlying these changes remain largely unknown. We know even less about how exposure to microgravity and chronically elevated CO_2 levels combine to affect the brain, cognition, and sensorimotor performance. Here, we investigated this issue using a well-established spaceflight analog, ‘head-down tilt bed rest’ (HDBR), combined with elevated levels of CO_2 to better simulate environmental conditions (i.e., microgravity and mild hypercapnia) experienced during spaceflight onboard the ISS.

HDBR studies have become the predominant model for simulating microgravity on Earth, and studying its effects on the human body (Hargens and Vico, 2016; Pavy-Le Traon et al., 2007). In an HDBR study, healthy participants continuously lay in bed with their head tilted below the level of the feet. HDBR mimics some of the effects of microgravity exposure including axial body unloading, reduced somatosensory inputs (Reschke et al., 2009), deconditioning (Hargens and Vico, 2016), headward fluid shifts and upward shift of the brain within the skull (Koppelmans et al., 2017b), sensorimotor behavioral dysfunction (Koppelmans et al., 2017a; Reschke et al., 2009), and changes in brain activity (Cassady et al., 2016; Liao et al., 2015, 2012; Yuan et al., 2018a, 2018b, 2016; Zhou et al., 2014). In contrast to previous bed rest studies, here we used "strict" HDBR. To keep the head tilted down at a 6° angle, subjects were not permitted to use a standard pillow.

In the current study, we used resting-state functional magnetic resonance imaging (rsfMRI) to assess how HDBR+CO_2 affects the brain's large-scale functional network architecture. The brain has the highest metabolic activity of any organ in the human body, and the majority of its energy is consumed while in a state of wakeful rest (Lord et al., 2013; Raichle, 2010a, 2010b). While at rest, several networks of distributed brain regions exhibit spontaneous, low frequency BOLD signal fluctuations. Resting-state fMRI is a method used to estimate correlations within these resting-state networks. Resting-state network topographies closely correspond to structural connectivity and therefore correlations within these networks are thought to reflect functional connectivity (FC) (Biswal et al., 1995; Fox et al., 2005).

Demertzi and colleagues (2016) investigated resting-state FC changes in a single cosmonaut following a 169-day mission on the ISS. They reported reduced intrinsic connectivity within the right insula and ventral posterior cingulate cortex as well as reduced FC between the cerebellum and motor cortex relative to pre-flight measures (Demertzi et al., 2016). HDBR studies simulating microgravity with larger sample sizes have examined how simulated microgravity in ambient air have reported resting-state functional connectivity increases involving somatomotor and vestibular cortices, the cerebellum, insular and cingulate cortices, parietal regions, and the thalamus (Cassady et al., 2016; Liao et al., 2015, 2013, 2012; Zeng et al., 2016; Zhou et al.,

2014). Connectivity increases may reflect increases in sensory weighting in microgravity or during HDBR, whereas connectivity decreases may be associated with reductions in use or reduced sensory weighting.

We have previously conducted a 70-day HDBR study in ambient air using a similar design, and an identical battery of sensorimotor and cognitive assessments to those employed here (Koppelmans et al., 2015). In our previous work, we have examined resting-state FC changes during HDBR in ambient air, and their associations with performance changes on identical behavioral assessments (Cassady et al, 2016). Methodology of the previous ambient air HDBR study differs with respect to the current HDBR+CO_2 study. First, the ambient air HDBR study did not employ strict bed rest; subjects were permitted to use a standard pillow (which altered the degree of head tilt) and subjects were permitted to raise their head while eating. Second, under NASA's directions, the previous ambient air HDBR study employed a different bed rest phase duration and a different testing timeline (Cassady et al, 2016). In the current study, we used similar analyses and identical regions of interests as Cassady et al (2016) to aid in drawing parallels between our results.

Lee et al (2019) contrasted the behavioral effects of HDBR+CO_2 compared to our previous ambient air HDBR study. In light of the differing bed rest phase durations, comparisons relied on the rates (slopes) of performance change over time. Lee et al. (2019) reported differential pre- to post-bed rest performance changes on three assessments: 1) response variability on a rod and frame test, 2) time to complete a digit symbol substitution test, and 3) time to complete the Functional Mobility Test. Here, since we were interested in the additive effects of elevated CO_2, we examined brain-behavioral associations for those behavioral measures that showed significantly different changes following HDBR+CO_2 compared to HDBR in ambient air. As published by Lee et al (2019), the HDBR+CO_2 group's performance on the digit symbol substitution task followed a learning curve throughout the study, providing clear evidence of practice effects but no discernable effect of the bed rest intervention. For this reason, we have omitted data from the digit symbol substitution test from our brain-behavioral analyses.

The aim of the current study was to investigate brain and behavioral effects of prolonged exposure to simulated microgravity and elevated CO_2 levels as a model of long-duration spaceflight onboard the International Space Station. Eleven subjects underwent 30 days of 6^o HDBR in 0.5% CO_2. Cognitive and sensorimotor tests were administered before, during, and after the HDBR+CO_2 intervention. Using both hypothesis-driven and hypothesis-free approaches, we examined: 1) time courses of resting-state FC changes from pre-, during-, to post-HDBR+CO_2, and 2) relationships between FC changes and behavioral changes associated with HDBR+CO_2. In light of previous work, we hypothesized that our 30-day HDBR+CO_2 intervention would alter resting-state FC involving sensorimotor brain areas, regions involved in multisensory integration, and brain areas within the default mode network (Cassady et al., 2016; Demertzi et al., 2016; Koppelmans et al., 2017a; Liao et al., 2015, 2012; Zhou et al., 2014). We also investigated FC changes involving visual brain areas as elevated CO_2 levels are hypothesized to contribute to the development of ophthalmic abnormalities and visual impairments in astronauts following long-duration spaceflight (Zwart et al., 2017). To determine the specificity of our findings, we conducted follow-up tests in which we compared the patterns of FC changes observed in the HDBR+CO_2 group to those of a HDBR control group, which underwent strict HDBR in standard ambient air.

METHODS

Participants

All data were collected at :envihab, the German Aerospace Center's medical research facility in Cologne, Germany. Prior to enrolment, all subjects passed psychological screening and an Air Force Class III equivalent physical examination. Subjects received monetary compensation for their participation. Study protocols were approved by the ethics commission of the local medical association (Ärztekammer Nordrhein) and institutional review boards at NASA, The University of Florida (HDBR+CO_2 and HDBR control). All subjects provided written informed consent at :envihab.

HDBR+CO_2 group

Twelve participants originally enrolled in the HDBR+CO_2 study. One participant withdrew from the study on the first day of bed rest. Eleven participants completed the HDBR+CO_2 study (6 males, 5 females; 25.3-50.3 years of age at study enrolment).

HDBR control group

Eight participants were included in a HDBR control group (6 males, 2 females; 27-46 years of age at study enrolment). Data from the HDBR control data were collected as part of a subsequent study which employed a 60-day bed rest phase. HDBR control data were also collected at :envihab approximately one year following data collection for the HDBR+CO_2 group.

Experimental Design

This experiment was part of the VaPER (Vision Impairment and Intracranial Pressure and Psychological :envihab Research) bed rest campaign. Subjects resided at :envihab for 58 consecutive days, during which they participated in several experiments. Our experiment consisted of 3 phases: a 14-day baseline data collection (BDC) phase, 30 days of strict 6^o head-down tilt bed rest phase with elevated CO_2 (HDBR+CO_2), followed by a 14-day recovery (R) phase (see Figure 1).

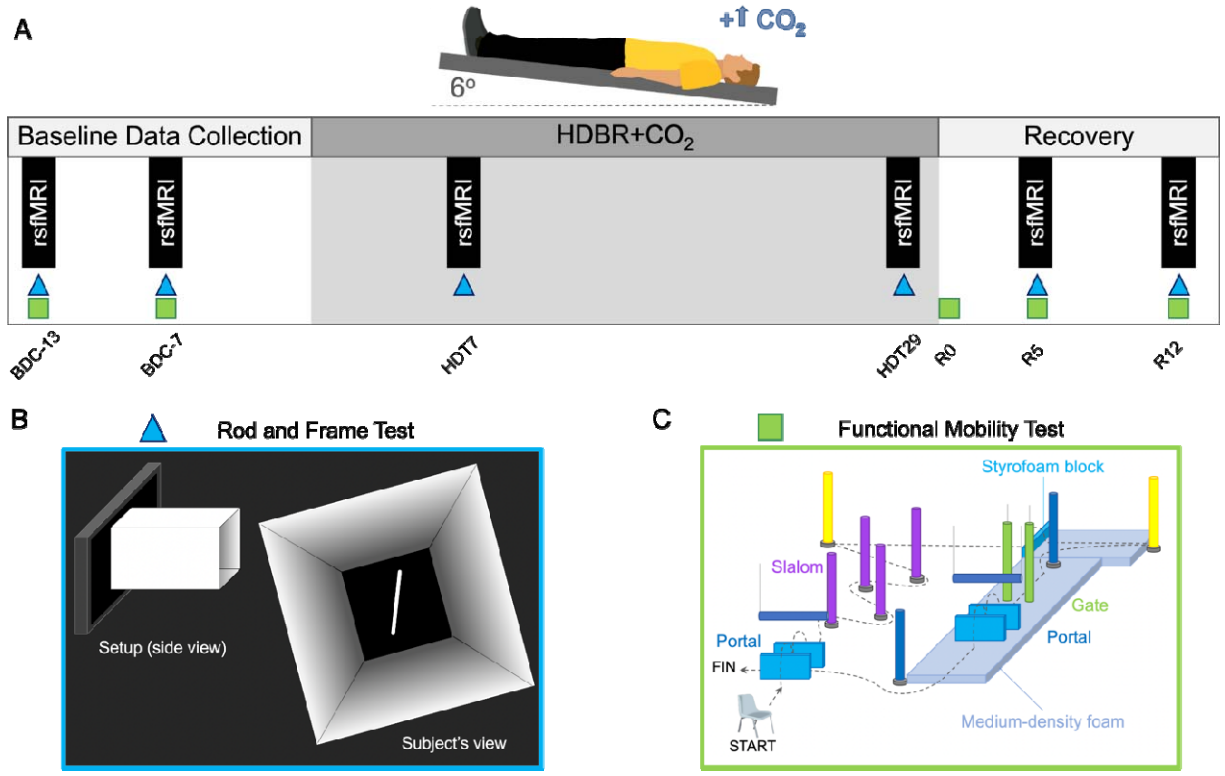

Figure 1. A) Subjects underwent a 15-day baseline data collection (BDC), 30 days of 6° head-down tilt bed rest with elevated carbon dioxide (HDBR+CO_2), followed by a 14-day recovery (R) phase. Resting-state fMRI scans occurred: 13 and 7 days before bed rest, on days 7 and 29 of the bed rest phase, and on the 6th day (R5) and 13th day (R12) during the recovery phase. **B)** Subjects performed a rod and frame test after each scan session. **C)** The Functional Mobility Test, an obstacle course, was administered twice during the baseline phase and three times following bed rest: on recovery days R0 (3 hours after first standing), R5, and R12.

Baseline Data Collection (BDC)

Subjects were admitted 15 days prior to bed rest for baseline data collection in standard ambient air (~0.04% CO_2). Subjects were ambulatory during the baseline phase, but were not permitted to leave the :envihab facility. Other than participating in study assessments, the subjects were not limited in their activities. Subjects slept in a horizonal (i.e., 0° tilt) position. For both groups, baseline resting-state fMRI scans and behavioral assessments (described below) occurred 13 and 7 days prior to bed rest (BDC-13 and BDC-7, respectively). Behavioral tests were performed approximately 3 hours after neuroimaging sessions. Baseline behavioral assessments (except

those requiring upright stance or locomotion) were performed while subjects laid in a 6° HDT position.

Head-down Tilt Bed Rest

All subjects remained in the HDT position 24 hours a day. They were instructed to have at least one shoulder in contact with the mattress at all times, and were not permitted to raise their head or prop themselves up. To keep the head tilted down at a 6° angle, subjects were not permitted to use a traditional pillow. Subjects were permitted to use a 5 cm tall support for the head and neck only when laying on their side (Laurie et al., 2019; 2020). No pillows were used when subjects laid on their back. Subjects were also not permitted to raise, contract or stretch their legs during the bed rest phase.

HDBR+CO_2 group

Subjects in the HDBR+CO_2 group underwent 30 consecutive days of strict 6° HDBR in elevated CO_2 (0.5%; 3.8 mmHg partial pressure of CO_2). Resting-state fMRI scans and behavioral assessments occurred on days 5 and 29 of the HDBR+CO_2 phase (HDT5 and HDT29, respectively). Behavioral assessments were conducted at the bedside approximately 3 hours after neuroimaging sessions while the subject was in the HDT position. The Functional Mobility Test, which required upright stance and locomotion, was not performed during the HDBR+CO_2 phase.

HDBR control group

Subjects in the HDBR control group underwent 60 consecutive days of strict 6° HDBR in standard ambient air. Resting-state fMRI scans occurred on days 29 (HDT29) and 58 of the bed rest phase. Here we analyzed HDBR control group resting-state fMRI data for the HDT29 session only since both underwent a HDT29 scan session.

Recovery (R)

Following bed rest, all subjects underwent a 14-day recovery (i.e., day R0 to day R13) phase in standard ambient air (~0.04% CO_2). Subjects were ambulatory, were not restricted in their activities, and slept in a horizonal (i.e., 0° tilt) position. Each subject received 1-hour rehabilitation sessions on days 3, 5, 7, 8, 9, and 11 of the recovery phase. Rehabilitation sessions

involved active stretching and exercise regimens using a Bosu® ball or coordination ladder to improve strength and coordination. For the HDBR+CO_2 group, resting-state fMRI scans were acquired on R5 and R12. The the rod and frame test were performed after scan sessions on R5 and R12 while subjects laid in 6^o HDT position. The Functional Mobility Test was performed 3 times during the recovery phase: on days R0 (approximately 3 hours after first standing after bed rest), R5, and R12. The group differences in bed rest duration preclude direct comparisons between the two groups during the recovery phase. We therefore omitted recovery phase resting-state fMRI data for the HDBR control group.

As part of NASA's standard measures assessments, blood draws were acquired 3 days prior to bed rest and on the first day after bed rest to calculate arterial partial pressure of carbon dioxide ($PaCO_2$). We predicted that $PaCO_2$ would increase from pre-to-post HDBR+CO_2. Changes in $PaCO_2$ were assessed using a one-tailed paired samples t-test.

Behavioral Assessments

Rod & Frame Test

The rod and frame test assesses the extent to which subjects rely on a visual frame of reference for their perception of true vertical. As shown in Figure 1 (lower left), a 60-cm-long white tunnel-like frame was affixed to a flat screen computer monitor. A white rod was displayed on the screen inside the square frame. Subjects laid on their side at the edge of the bed and the end of the frame was positioned around their face to occlude any visual cues from the surrounding room. Subjects were then presented with random tilts of the rod and ±18° frame tilts for each trial, and they used a handheld controller to align the rod to Earth vertical (i.e., 0^o tilt). Each response was scored based on the deviation, in degrees, between perceived and true vertical. The primary outcome presented here is response consistency which refers to the within-subject variability of scores for a given rod/frame tilt combination. Since higher values reflect greater variability, here we refer to this measure as response variability.

Functional Mobility Test

Subjects' locomotor function was assessed using the Functional Mobility Test (Figure 1, lower right). This test requires subjects to navigate an obstacle course by performing whole-body movements similar to those required to exit a vehicle after long-duration spaceflight (Mulavara et al., 2010; Koppelmans et al. 2013). The first half of the Functional Mobility Test was built on a hard surface while the second half was built on a medium-density foam floor. The foam base was used to reduce the reliability of proprioceptive input (Mulavara et al., 2010) and increase reliance on vestibular cues (Jeka et al., 2004). This course was comprised of 1) foam pylons arranged in a slalom pattern, requiring quick changes in heading direction, 2) "portals" consisting of a horizontally-hung foam obstacle between 2 styrofoam blocks which required subjects to bend at the waist and balance on one foot while stepping over the Styrofoam blocks, 3) a Styrofoam block located at the transition point between the hard floor and foam base, requiring subjects to balance on one foot on the unstable foam while clearing the Styrofoam block, and 4) a "gate" consisting of 2 vertically-hung pylons through which subjects entered sideways (i.e., shoulder first). Subjects started in a seated position. They were instructed to walk quickly and safely through the course without touching any obstacles. Here we present the time to complete the first of 10 trials as this measure is most sensitive to mobility changes.

Since the aim of the current study was to investigate brain and behavioral effects of our HDBR+CO_2 intervention, we examined behavioral changes from immediately pre- to post-HDBR+CO_2, as this is where the behavioral changes are most evident.

MRI Image Acquisition

During all MRI scan sessions, a foam wedge was used to maintain the subject's body in the 6° HDT position, but the head was horizontal in the MRI coil. For subjects in the HDBR+CO_2 group only, a mask and tank system was used to maintain the 0.5% CO_2 level throughout scan sessions during the bed rest phase.

All neuroimaging data were acquired on a 3-Tesla Siemens Biograph mMR scanner. T1-weighted anatomical images were collected using a MPRAGE sequence with the following parameters: TR = 1900 ms, TE = 2.44 ms, flip angle = 9°, FOV = 250 x 250 mm, matrix = 512 x 512, voxel size = 0.5 x 0.5 mm, 192 sagittal slices, slice thickness = 1 mm, slice gap = 0.5 mm. Whole-brain functional data were acquired using a T2*-weighted EPI sequence with the

following parameters: TR = 2500 ms, TE = 32 ms, flip angle = 90°, FOV = 192 x 192 mm, matrix = 64 x 64, voxel size = 3 x 3 x 3.5 mm, slice thickness = 3.5mm, 37 axial slices, duration = 7 minutes. During the resting-state scan, participants were instructed to remain awake with their eyes open, fixate a red circle, and not think about anything in particular.

Image Preprocessing

Neuroimaging data analyses were performed using the Statistical Parametric Mapping 12 software (SPM12; www.fil.ion.ucl.ac.uk/spm) and the CONN toolbox version 18a (Whitfield-Gabrieli and Nieto-Castanon, 2012) implemented in Matlab 2018b. Image preprocessing was identical for the HDBR+CO_2 group and HDBR control group. Functional image preprocessing included spatial alignment to the first volume, slice timing correction, coregistration, and normalization with resampling to 2 mm isotropic voxels. Structural images were segmented into gray matter, white matter, and cerebrospinal fluid (CSF) tissue maps, and normalized to Montreal Neurological Institute (MNI) standard space.

To improve cerebellar normalization, we used CERES to segment the cerebellum from each subject's anatomical image (Romero et al., 2017). CERES is an automated pipeline that uses a segmentation method called Optimized PatchMatch Label fusion (for details see Romero et al., 2017). CERES has been shown to yield more accurate cerebellar segmentations compared to other tools including the SUIT toolbox (Carass et al., 2018). CERES was used to segment the cerebellum from each native space anatomical scan. Generated cerebellar masks were used to extract the cerebellum from each subject's session-wise T1 and coregistered functional images. The cerebellums extracted from functional and structural images were then normalized to the SUIT space template. The SUIT template was used because it retains more anatomical detail within the cerebellum compared to whole brain MNI templates, resulting in improved normalization for functional MRI (Diedrichsen, 2006).

Whole-brain functional images were spatially smoothed using a 5 mm full width at half maximum (FWHM) Gaussian kernel. The cerebellums extracted from functional scans were

spatially smoothed using a 2 mm FWHM Gaussian kernel. A smaller smoothing kernel was used for the cerebellums so as to reduce smoothing across lobules and tissue types.

Image Denoising

Since measures of resting-state FC are known to be influenced by head motion (Van Dijk et al., 2012), we used the ARTifact detection tool (ART; http://www.nitrc.org/projects/artifact_detect) to detect and reject motion artifacts. Within each resting-state run, a volume was deemed an outlier if the subject's composite movement exceeded 0.9 mm or if the global mean intensity of the volume exceeded 5 standard deviations from the mean image intensity of the run. This corresponds to the intermediate default motion thresholds in the CONN toolbox (Whitfield-Gabrieli and Nieto-Castanon, 2012). ART generated a "scrubbing" regressor which identified outlier volumes. For the HDBR+CO_2 group, the following number of volumes (± SD, range) were detected as outliers at each of the time points: BDC-13: 2.4 ± 3.3 SD, range=0-9; BDC-7: 1.5 ± 1.8 SD, range=0-4; HDT7: 0.36 ± 1.2 SD, range=0-4; HDT29: 0 outlier volumes; R5: 0.55 ± 1.8 SD, range=0-6; R12: 0.63 ± 1.3 SD, range=0-4. As 164 volumes were acquired during each resting-state run, less than 6% of the original data points (i.e., 9/164 volumes) were identified as outliers and regressed out across subjects and sessions. A repeated measures ANOVA followed by Bonferroni post-hoc tests revealed no statistically significant main effect of session on the number of outlier volumes [Wilks' $F(5,6)=1.426$, $p=0.336$] for the HDBR+CO_2 group. Including subject-wise regressors modelling the number of outlier volumes for each resting-state fMRI run resulted in qualitatively similar results. Similarly, for the HDBR control group, a repeated measures ANOVA followed by Bonferroni post-hoc tests revealed no significant main effect of session on the number of outlier volumes [Wilks' $F(2,6)=0.741$, $p=0.516$].

Resting-state fMRI data are also influenced by noise arising from physiological fluctuations, primarily cardiac pulsations and respiration, which can exhibit spatial and spectral overlap with resting-state networks (Cole et al., 2010). We used the anatomical component-based noise correction (aCompCor) method to denoise our data (Behzadi et al., 2007). This method uses a principal components analysis approach to estimate noise signals in the white matter and CSF. For each session, the participant's anatomical image was segmented into white matter and CSF masks. Resulting masks were eroded by one voxel to reduce partial volume effects, and were

then applied to unsmoothed resting-state functional images. Unsmoothed functional images were used to avoid smoothing the BOLD signal across neighboring brain areas and different tissue types. BOLD signals were then extracted from the white matter and CSF used as noise regions of interest (ROIs) in a principal components analysis. The resulting significant components modelled the influence of noise as a voxel-wise linear combination of multiple estimated sources. For each run, 5 principal components were extracted for each of the white matter and CSF noise ROIs, and were included as nuisance regressors in our first-level GLM.

Each preprocessed resting-state run was denoised by regressing out confounding effects of head motion (6 head motion parameters and their 6 first-order temporal derivatives), 5 principal components modelling estimated noise from the white matter, 5 principal components modelling estimated noise from the CSF, and a "scrubbing" regressor modelling outlier volumes within the run. The resulting residuals were band-pass filtered between 0.008–0.09 Hz (Biswal et al., 1995; Damoiseaux et al., 2006) prior to being used in subject-level analyses.

Subject-level analyses

We used two approaches to examine connectivity changes associated with HDBR+CO_2: a hypothesis-based seed-to-voxel analysis and a hypothesis-free voxel-to-voxel analysis.

Seed-to-voxel analysis

For our seed-to-voxel analyses, we selected 13 *a priori* seed regions of interest (ROIs). We hypothesized that our HDBR+CO_2 intervention would induce functional changes involving sensorimotor brain areas, regions involved in multisensory integration, and brain areas within the default mode network (Cassady et al., 2016; Demertzi et al., 2016; Koppelmans et al., 2017a; Liao et al., 2015, 2012; Zhou et al., 2014; Zeng et al., 2016). We used the same ROI coordinates as used in our previous resting-state fMRI study using an ambient air HDBR intervention (Cassady et al., 2016). Elevated CO_2 levels are hypothesized to be one of the environmental factors contributing to the development of ophthalmic abnormalities and visual impairments in astronauts following long-duration spaceflight (Zwart et al., 2017). Therefore, we also included ROIs located within primary visual cortex and frontal eye field, the coordinates of which were

411 determined using the automatic anatomic labeling (AAL) atlas included in the CONN toolbox.
412 Table 1 shows coordinates for ROIs used in our seed-to-voxel analyses.
413

Regions of Interest (ROIs)	**MNI Coordinates**		
	x	***y***	***z***
R premotor cortex (PMC)	26	-10	55
R middle frontal gyrus (MFG)	30	-1	43
L primary motor cortex (M1)	-38	-26	50
L putamen	-28	2	4
L insular cortex	-41	12	-9
R vestibular cortex	42	-24	18
L frontal eye field (FEF)	-27	-9	64
L posterior cingulate cortex (PCC)	-12	-47	32
R posterior parietal cortex (PPC)	28	-72	40
R superior posterior fissure	24	-81	-36
L primary visual cortex (V1)	-10	-70	10
R cerebellar lobule V	16	-52	-22
R cerebellar lobule VIII	20	-57	-53

414
415 **Table 1.** Regions of interest (ROIs) and their coordinates used for seed-to-voxel analyses. L, left;
416 R, right.
417
418 ROIs included all voxels within a 4-mm-radius sphere centered on the ROI coordinates. We first
419 extracted the time series from unsmoothed functional data within each ROI. For ROIs located in
420 the cerebrum, ROI time series were drawn from the whole brain unsmoothed functional images
421 (source image). For ROIs located in the cerebellum, ROI time series were drawn from the
422 unsmoothed cerebellums extracted from functional images (source image). We then computed
423 the spatial average of the BOLD time series across all voxels with the ROI.
424
425 We estimated FC between each ROI and the rest of the brain or within the cerebellum. For each
426 ROI, we computed (bivariate) Pearson's correlation coefficients between the mean ROI time
427 series and the time series of every other voxel in the smoothed whole brain functional and within

the cerebellum (i.e., smoothed cerebellums extracted from functional scans). Correlation coefficients were then Fisher Z-transformed to improve their normality. This procedure was performed for each of the subjects' six resting-state scans separately.

Voxel-to-voxel analyses

We also used hypothesis-free voxel-to-voxel analyses. This allowed us to identify connectivity changes without restricting our analyses to our *a priori* selected ROIs. Here we examined changes in Intrinsic Connectivity Contrast (ICC), a measure which utilizes graph theory metrics to estimate global connectivity pattern strength (Martuzzi et al., 2011). This analysis involved computing (bivariate) Pearson's correlation coefficients between the time course of each voxel with the time series of every other voxel in the brain (or within the cerebellum). The root mean square of each correlation was then computed. Correlation coefficients were then Fisher Z-transformed to improve their normality. This yielded one ICC map per run, each reflecting the connectivity strength (i.e., magnitude) at each voxel.

Group-level Functional Connectivity Analyses

Time Course of Functional Connectivity Changes with HDBR+CO_2

In this study, we were interested in the brain's gradual adaptation to prolonged simulated microgravity and chronic CO_2 elevation as opposed to the acute effects of elevated CO_2 exposure. For both our seed-to-voxel and voxel-to-voxel analyses, we used the longitudinal model shown in Figure 2 to assess the time course of FC changes from pre-, during-, to post-bed rest. Our aim was to identify those brain regions that exhibited stable FC across the 2 baseline time points, then showed a gradual change in FC during HDBR+CO_2, followed by a gradual return to baseline over the 2 post-bed rest time points. In this way, subjects served as their own controls.

The HDBR+CO_2 group and HDBR control group differed in bed rest duration (30 vs. 60 days) and data collection timeline (6 vs 5 sessions). This precluded direct comparison of the groups in our GLM. In light of this, we performed GLM analyses on the HDBR+CO_2 group data only. Based on the results of these analyses, we performed follow-up assessments using resting-state fMRI data from the HDBR control group (detailed below).

For these analyses, our hypothesized model weights as a within-subjects contrast in our general linear model (GLM). The between-subjects regressor of interest was the grand mean. Age and sex were included as between-subjects covariates of no interest. Our analysis is analogous to that used by Cassady et al (2016). An uncorrected voxel threshold of $p < 0.001$ was set, and results were considered statistically significant at a cluster-level threshold of $p < 0.05$ (two-tailed), corrected for multiple comparisons according to the false discovery rate (FDR) method.

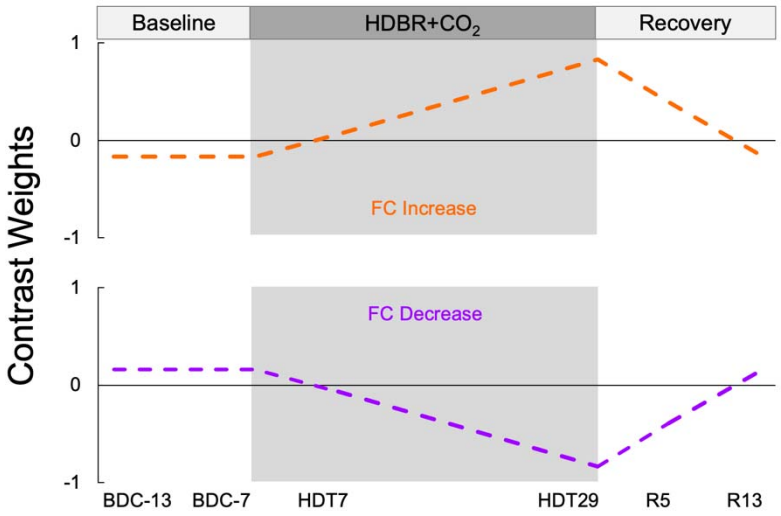

Figure 2. Contrast models used to assess time course of FC changes of the HDBR+CO_2 group. Contrast weights used in the HDBR+CO_2 group analyses. The gray shaded region indicates the HDBR+CO_2 phase. The contrast in orange models a gradual FC increase during bed rest followed by a gradual FC decrease back to baseline level following bed rest. The contrast in purple models a gradual FC decrease during bed rest followed by a gradual FC increase back to baseline level following bed rest. BDC, baseline data collection; HDBR+CO_2, head-down tilt bed rest with elevated carbon dioxide; R, recovery.

Time Course of Functional Connectivity Changes for HDBR control group

We performed follow-up assessments using the resting-state fMRI data from the HDBR control group. This was done to examine if the FC changes identified by our HDBR+CO_2 longitudinal analyses were due to undergoing strict HDBR alone or due to the combination of strict bed rest and elevated CO_2. We used HDBR control group resting state data from BDC-13, BDC-7, and

HDT29 sessions as the both groups underwent scans on these days. For each significant cluster identified by our HDBR+CO_2 longitudinal analysis, we generated a binary mask of the cluster. The cluster mask was used to extract FC or ICC values for each subject in the HDBR control group for sessions BDC-13, BDC-7, and HDT29. If a cluster resulted from a seed-to-voxel analysis, we extracted average FC values between the ROI and all voxels within the cluster mask. If a cluster resulted from a voxel-to-voxel analysis, we extracted average ICC values across all voxels within the cluster mask.

We then performed a split-plot ANOVA using IBM® SPSS® Statistics 21 to compare the time course of connectivity changes across BDC-13, BDC-7 and HDT29 between the HDBR+CO_2 group and the HBDR control group. If the connectivity changes observed in the HDBR+CO_2 group from BDC-13 to HDT29 are indeed due to the combination of strict HDBR and elevated CO_2, it follows that the time courses of connectivity changes will differ between the two groups (i.e., a significant group x session interaction). However, if the connectivity changes observed in the HDBR+CO_2 do not differ from those of the HDBR control group, then this would suggest that the connectivity change was a result of undergoing strict HDBR.

Behavioral Analyses

We have recently examined cognitive and motor performance alterations following 6^o HDBR+CO_2 compared to 6^o HDBR with ambient air (Lee et al., 2019). These two bed rest studies employed an identical battery of behavioral tests (Koppelmans et al., 2015). Since we were interested in the additive effects of elevated CO_2, here we examined only those behavioral measures that showed significantly different changes following HDBR+CO_2 compared to ambient air HDBR. Differential performance changes were found for the following behavioral measures: i) response variability on the rod and frame test (referred to as response consistency in previous work), and ii) time to complete the full Functional Mobility Test.

Here we tested if pre- to post-HDBR+CO_2 FC changes were associated with behavioral changes (i.e., a change-change correlation). For each of the behavioral measures above, we computed each subject's change in behavior from the last baseline time point (BDC-7) to the end of bed rest (HDT29; R0 for the Functional Mobility Test only).

Associations Between Functional Connectivity and Behavior Changes

We then performed group-level GLM analyses to test if pre- to post-HDBR+CO_2 FC changes were associated with behavioral changes. Here we examined FC from 7 days before bed rest (BDC-7) to day 29 of bed rest (HDT29). A separate analysis was performed for each behavioral test. For these analyses, we calculated the change in each subject's performance from before bed rest to the end of bed rest. The regressor of interest for our between-subjects contrast modeled the performance changes across subjects. Subject age, sex, and the grand mean were included as covariates of no interest. Our within-subjects contrast modeled the change in FC from pre- to post-bed rest. These analyses allowed us to examine those areas of the brain in which FC changes following HDBR+CO_2 were significantly associated with performance changes. An uncorrected voxel threshold was set at $p < 0.001$, and results were thresholded at a FDR-corrected significance level of $p < 0.05$ (two-tailed, cluster-wise).

In total, 56 tests were conducted using GLMs (13 seed-to-voxel and 1 voxel-to-voxel analyses conducted for the time course analysis and each of the 3 brain-behavior associations). We used the Benjamini-Hochberg procedure to control the false discovery rate at 0.05 (Benjamini and Hochberg, 1995). Cluster-level uncorrected p value obtained by each GLM analysis were submitted to Benjamini and Hochberg's FDR procedure with αFDR = 0.05 (Chumbley et al., 2010). A cluster was considered statistically significant if its uncorrected cluster size $p < 0.00089$ (i.e., (1/56) x 0.05).

RESULTS

A paired samples t-test revealed a small but significant increase in $PaCO_2$ from pre- (41.4 mmHg) to post- (43.4 mmHg) HDBR+CO_2 ($t(10)=2.16$, $p=0.028$, one-tailed).

Time Course of Functional Connectivity Changes with HDBR+CO_2

Seed-to-voxel analyses

Seed-to-voxel analyses revealed that right vestibular cortex exhibited increases in FC with right cerebellar crus I and II during HDBR+CO_2, followed by a reduction in connectivity following bed rest (Figure 3A). A split plot ANOVA examining group differences in longitudinal FC changes revealed a non-significant group x session interaction ($F(2,34)=2.519$, $p=0.095$) although there was a trend.

Our ROI in right premotor cortex exhibited FC increases with bilateral primary visual cortex (V1) during HDBR+CO_2, which decreased after bed rest (Figure 3B). A split-plot ANOVA revealed a significant group x session interaction on FC values ($F(2,34)=4.485$, $p=0.019$). This indicated differential patterns of FC changes from the baseline phase to the HDT29 session in which the HDBR+CO_2 group exhibited a greater increase during the bed rest phase.

The ROI in left putamen showed increased FC with clusters in right superior and middle frontal gyrus during HDBR+CO_2, which reversed after bed rest (Figure 3C). The time course of FC for the HDBR+CO_2 group was significantly different from that of the HDBR control ($F(2,34)=4.049$, $p=0.026$) such that the HDBR+CO_2 showed greater FC increases during bed rest. The ROI in left putamen also exhibited FC decreases between left superior frontal gyrus, bilateral lateral occipital cortices, and bilateral posterior cingulate cortices during bed rest, followed by a reversal post-bed rest (Figure 3C). A split-plot ANOVA revealed a significant group x session interaction on FC values ($F(2,34)=3.961$, $p=0.028$), suggesting that FC decreases during bed rest were greater for the HDBR+CO_2 group.

The ROI in right middle frontal gyrus exhibited FC decreases with a distributed network during bed rest including bilateral insular cortices, left primary somatosensory cortex, left lateral occipital cortex, right supplementary motor area, and right posterior cingulate cortex (Figure 3D). However, the clusters in left primary somatosensory cortex and left lateral occipital cortex did not survive post hoc Benjamini-Hochberg FDR correction. Consequently, FC values from these 2 clusters were omitted from the FC plot on the far right of Figure 3D and omitted from our split-plot ANOVA. The longitudinal pattern of FC changes significantly differed between the

two groups ($F(2,34)=3.92$, $p=0.029$) such that the HDBR+CO_2 showed greater FC decreases during bed rest.

Finally, left insula showed decreased FC with right SFG, right SPL, and cerebellar crus I and II, followed by a reversal after bed rest (Figure 3E). Cluster coordinates and statistics are presented in Table 2. A split-plot ANOVA revealed a significant group x session interaction on FC values ($F(2,34)=11.046$, $p= 0.0002$) demonstrating that the HDBR+CO_2 group exhibited greater FC decreases from the baseline phase to HDT29 compared to the HDBR control group.

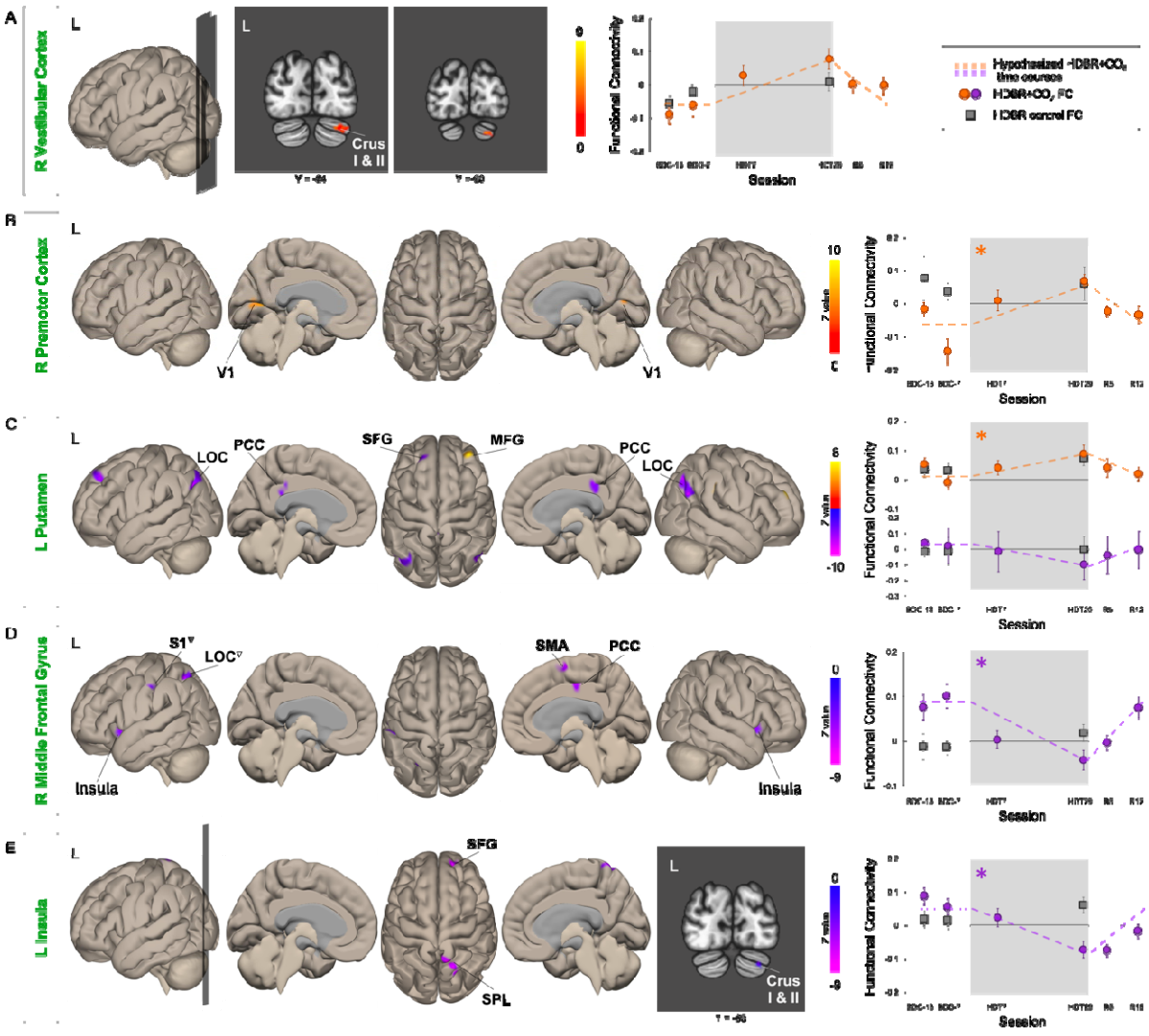

Figure 3. Time Course of Functional Connectivity Changes with HDBR+CO_2. Results of our seed-to-voxel analyses, with each ROI indicated in green font. Significant clusters that exhibited

FC increases during HDBR+CO_2 followed by a post-bed rest reversal are shown in warm colors. Significant clusters that exhibited FC decreases during HDBR+CO_2 followed by a post-bed rest reversal are shown in purple. Plots on the right represent session-wise functional connectivity values averaged across all clusters. Results from the HDBR+ CO_2 group are indicated by colored circles. FC values across all clusters were extracted from the HDBR control group and are indicated by grey squares. ∇ indicates a cluster that did not survive the post hoc Benjamini-Hochberg FDR correction. * indicates a significant group x session interaction. Error bars represent standard error. L, left; R, right; FC, functional connectivity; BDC, baseline data collection; HDT, head-down tilt; R, recovery.

	ROI	Target cluster	MNI Coordinates			T value	Cluster size	Cluster-level uncorr p
			x	*y*	*z*			
Increases	R vestibular cortex	R cerebellar crus I & II	26	-86	-26	8.45	36	0.00050
	R premotor cortex	Bilateral primary visual cortex	16	-78	8	6.99	48	0.00005
	L putamen	R middle frontal gyrus	36	46	26	9.18	61	0.000008
Decreases	L putamen	L lateral occipital cortex	-40	-64	32	-9.59	60	0.000010
		R lateral occipital cortex	42	-68	40	-8.18	29	0.0008
		Posterior cingulate gyrus	0	-36	36	-7.72	51	0.000031
	R middle frontal gyrus	L insular cortex	-28	10	10	-10.62	63	0.000008
		L lateral occipital cortex∇	-26	-58	52	-7.72	25	0.001739
		R insular cortex	42	10	-2	-9.55	39	0.000194
		R posterior cingulate gyrus	10	-16	42	-9.29	39	0.000016
		L postcentral gyrus∇	-40	-30	38	-7.45	24	0.00174
		Supplementary motor area	0	-2	62	-9.24	59	0.000013
	L insular cortex	R cerebellar crus I & II	26	-88	-32	-12.15	62	0.000021
		R lateral occipital cortex	12	-52	68	-7.08	45	0.000164
		R superior frontal gyrus	16	52	28	-8.07	44	0.000187

606 **Table 2**. Significant clusters from our seed-to-voxel analyses assessing FC change time courses.
607 Top rows indicate ROIs and clusters that exhibited FC increases during HDBR+CO_2 followed by
608 FC decrease during the post-bed rest recovery period. Bottom rows indicate ROIs and clusters
609 that exhibited FC decreases during HDBR+CO_2 then FC increase following bed rest. Cluster size
610 refers to the number of voxels in each cluster. Cluster size uncorr p refers to uncorrected cluster
611 size *p*-values. ∇ indicates a cluster that did not survive the post hoc Benjamini-Hochberg FDR
612 correction. L, left; R, right; ROI, region of interest; uncorr, uncorrected.
613
614 *Voxel-to-voxel analyses*
615 Voxel-to-voxel analyses revealed a significant cluster within right primary visual cortex.
616 Intrinsic connectivity contrast (ICC) within right V1 decreased during HDBR+CO_2 then
617 increased during the post-bed rest recovery phase (Figure 4, Table 3). A split-plot ANOVA
618 examining group differences in longitudinal ICC changes revealed a non-significant group x
619 session interaction (F(2,34)=2.172, p=0.130) although there was a trend.
620
621

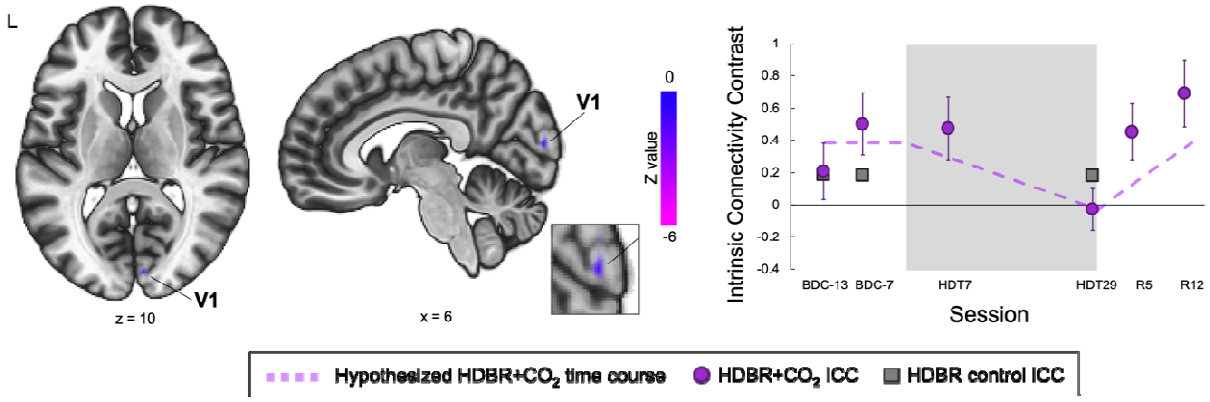

622
623 **Figure 4. Time Course of Intrinsic Connectivity Contrast (ICC) with HDBR+CO_2.** Results
624 of our voxel-to-voxel analyses. A cluster in right primary visual cortex exhibited decreased
625 connectivity during HDBR+CO_2 followed by a reversal during the recovery phase (colored
626 circles). ICC values across all clusters were extracted from the HDBR control group and are
627 indicated by grey squares. The inset shows an enlarged sagittal view of the cluster. The plot on
628 the right reflects average Fisher Z-transformed intrinsic connectivity contrast (ICC) estimates
629 across all subjects. Error bars represent standard error. Dashed lines represent our hypothesized
630 longitudinal model. L, left; BDC, baseline data collection; HDT, head-down tilt; R, recovery.

Cluster	MNI Coordinates			T value	Cluster size	Cluster-level uncorr p
	x	*y*	*z*			
R primary visual cortex	6	-88	10	-9.85	46	0.00001

Table 3. Significant cluster from our voxel-to-voxel analyses assessing FC change time courses. Cluster size refers to the number of voxels in each cluster. Cluster-level uncorr p refers to uncorrected cluster size *p*-values. R, right; uncorr, uncorrected.

Associations Between Functional Connectivity and Behavior Changes

Lee and colleagues (2019) recently contrasted behavioral changes during our HDBR+CO_2 intervention compared to our previous ambient air HDBR study. Here we examined brain-behavior associations for those behavioral measures that exhibited differential changes during HDBR+CO_2 compared to our previous ambient air HDBR study. Lee et al. reported that response variability on the rod and frame test remained consistent during HDBR in ambient air, but decreased during HDBR+CO_2. While both interventions resulted in slowed performance on the Functional Mobility Test, the degree of slowing was greater for the HDBR+CO_2 group. Therefore, subjects who underwent the HDBR+CO_2 intervention exhibited improved consistency of visual orientation perception compared to the ambient air HDBR group. However, the HDBR+CO_2 group exhibited greater mobility impairments compared to the ambient air HDBR group (Lee et al., 2019). Figure 5 shows the evolution of each of the behavioral measures across all sessions for the HDBR+CO_2 group only.

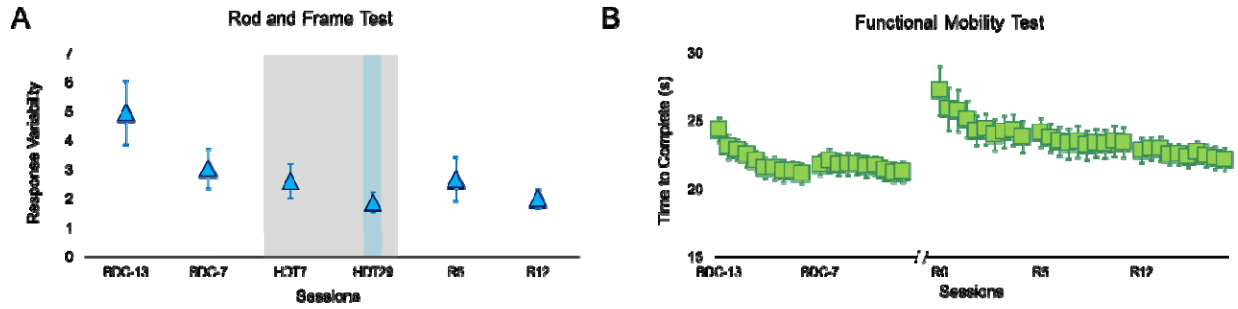

Figure 5. Performance on behavioral assessments. Session-wise group average of response variability on the rod and frame test **(A)** and time to complete each trial of the Functional Mobility Test **(B)**. Error bars represent SEM. The gray shaded region indicates the HDBR+CO_2 phase. Colored bars indicate data used for pre- to post-bed rest performance comparisons. BDC, baseline data collection; HDT, head-down tilt; R, recovery.

We also examined how pre- to post-bed rest FC changes related to behavioral changes across subjects in the HDBR+CO_2 group.

Rod and Frame Test

On average, subjects' responses showed reduced variability (i.e., increased consistency) during HDBR+CO_2 (Figure 5A). However, as shown in scatterplots in Figure 6, individual subjects differed in the direction and extent of response variability changes with HDBR+CO_2. We found that post-bed rest FC decreases between left frontal eye field (FEF) and right lateral occipital cortex (LOC) were associated with decreased response variability (i.e., increased consistency) following bed rest (see Figure 6A). FC decreases between left insula and left primary somatosensory cortex (S1) were also associated with decreases in response variability. Finally, we also observed a relationship between connectivity changes within the default mode network and performance changes on the rod and frame test (Figure 6C). Post-bed rest FC decreases between left posterior cingulate cortex, left superior frontal gyrus, and right superior parietal lobule (SPL) were associated with decreases in response variability. The scatterplots on the right show the relationship between pre-to-post-HDBR+CO_2 performance changes, which were used as the regressor of interest, and FC changes across subjects. Scatterplots are intended for illustrative purposes. A further correlation analysis was not performed because the nonindependence of such an analysis would inflate the effect size (Poldrack & Mumford, 2009). Cluster coordinates and statistics are presented in Table 4. Results were qualitatively similar if we used the subjects' slope of behavioral change across BDC-7, HDT7, and HDT29 as our regressor of interest.

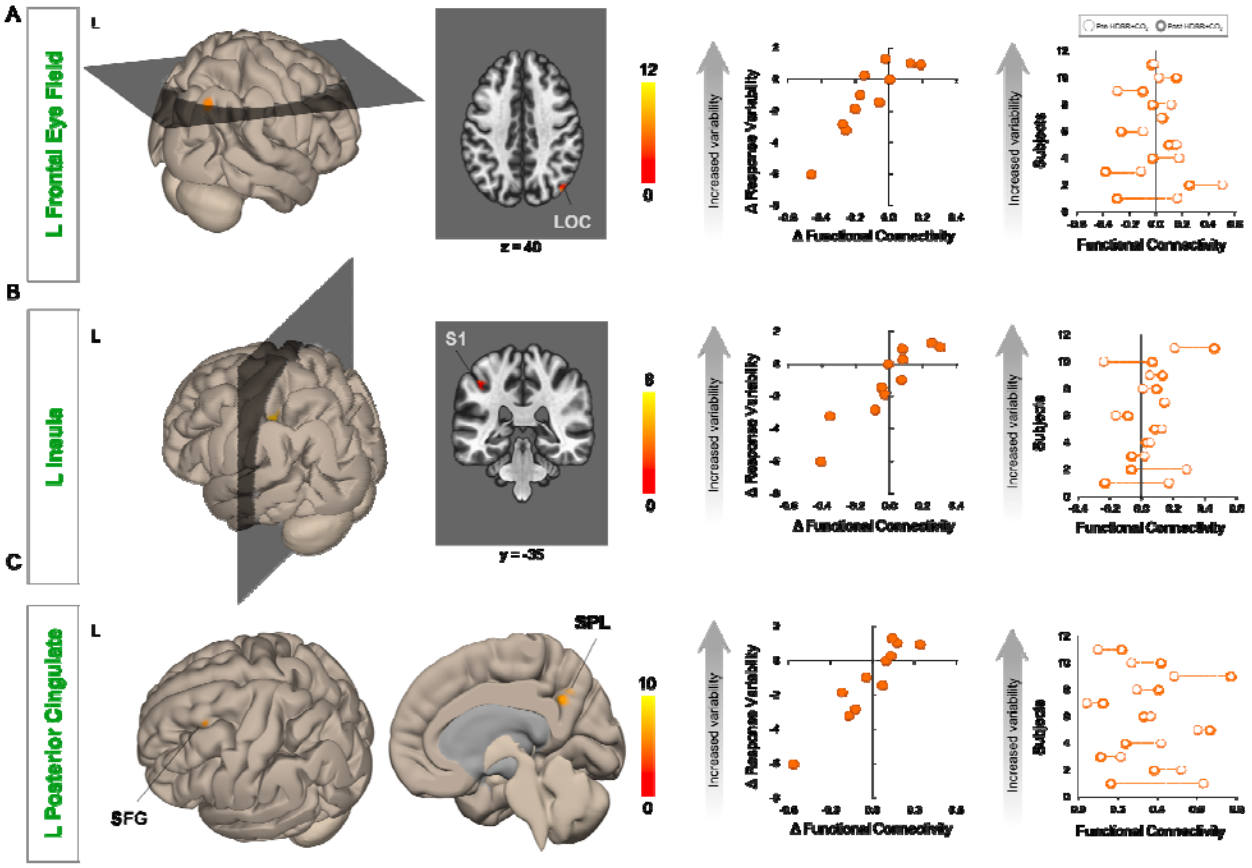

Figure 6. Pre- to Post-HDBR+CO_2 changes in FC and response variability on the rod and frame test. Results of our seed-to-voxel analyses, with each ROI indicated in green font. Columns 1 and 2 show clusters that exhibited FC increases that were significantly associated with response variability increases from pre- to post-bed rest. Changes in response variability are plotted against functional connectivity changes in column 3 to illustrate the direction of the effect. The plot in column 4 shows subject-wise functional connectivity values before and after HDBR+CO_2. Subjects are rank-ordered along the y-axis according to increasing response variability. L, left; LOC, lateral occipital cortex; S1, primary somatosensory cortex; SFG, superior frontal gyrus; SPL, superior parietal lobule; BDC, baseline data collection; HDT, head-down tilt; FC, functional connectivity; HDBR+CO_2, head-down tilt bed rest with elevated CO_2.

ROI	Target cluster	MNI Coordinates			T value	Cluster size	Cluster-level uncorr p
		x	*y*	*z*			
L frontal eye field	R lateral occipital cortex	42	-76	40	12.99	48	0.000029
L insular cortex	L postcentral gyrus	-40	-36	48	12.57	50	0.00028
L posterior cingulate cortex	L superior frontal gyrus	-34	12	64	9.26	38	0.000123
	R superior parietal lobule	6	-54	36	9.37	35	0.000199

Table 4. MNI coordinates of clusters that showed post-bed rest FC changes that were significantly associated with changes in response variability on the rod and frame test. Cluster size refers to the number of voxels in each cluster. Cluster-level uncorr p refers to uncorrected cluster size *p*-values. ROI, region of interest; L, left; R, right; uncorr, uncorrected.

Functional Mobility Test

All subjects exhibited slowing on the Functional Mobility Test (i.e., increases in completion times) following HDBR+CO_2 (see Figures 5C, Figure 8), however, the extent of slowing varied across subjects. Post-bed rest FC increases between left primary motor cortex and left visual area V5 were associated with greater slowing on the Functional Mobility Test (Figure 8A). FC increases between right premotor cortex and left cerebellar crus I were also associated with greater slowing on the Functional Mobility Test following bed rest (see Figure 8B). Post-bed rest FC decreases between left primary visual cortex and right inferior parietal lobule were associated with greater slowing on the Functional Mobility Test. In contrast, subjects who exhibited increased FC between these areas showed less slowing. Cluster statistics are summarized in Table 6.

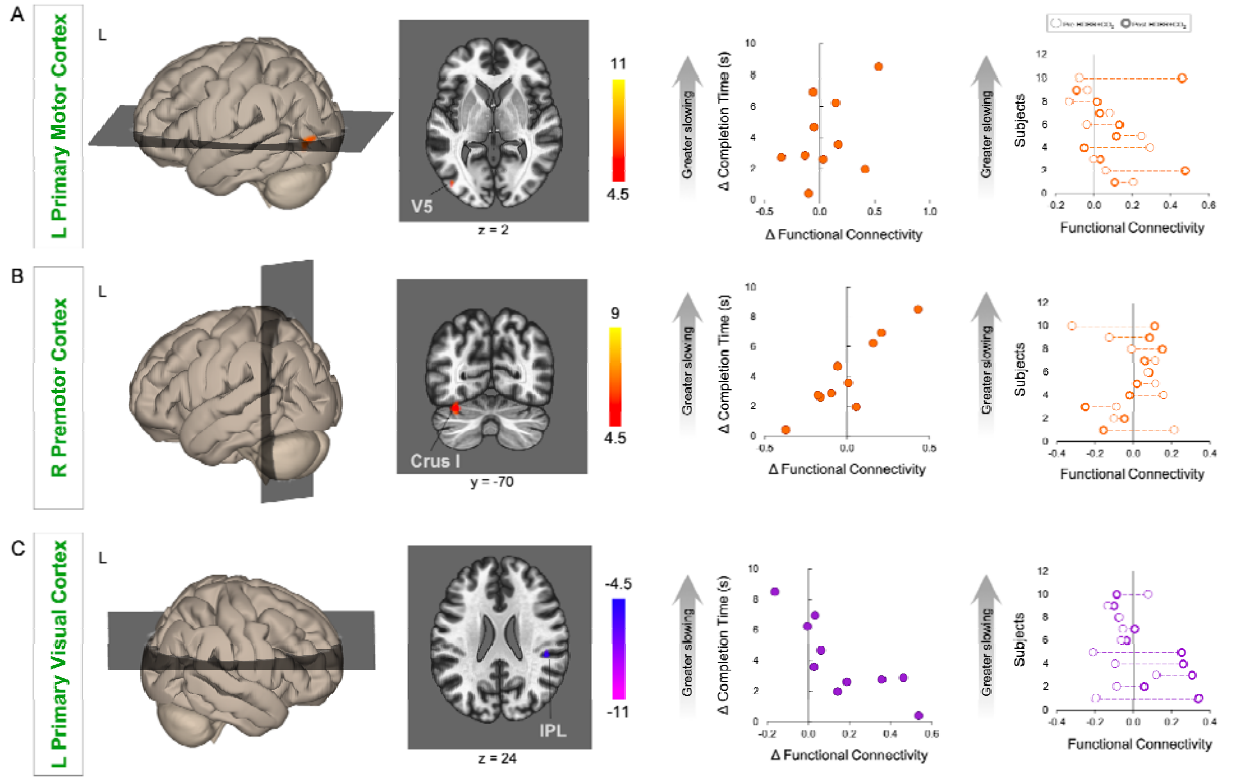

Figure 7. Pre- to Post-HDBR+CO_2 changes in FC and time to complete the Functional Mobility Test. Results of our seed-to-voxel analyses, with each ROI indicated in green font. Clusters that exhibited post-HDBR+CO_2 FC increases that were significantly associated with increases in Functional Mobility Test completion time. Changes in completion time are plotted against functional connectivity changes in column 3 to indicate the direction of the effect. The plot on the far right shows subject-wise functional connectivity values before and after HDBR+CO_2. Subjects are rank-ordered along the y-axis according to increasing slowing of mobility. L, left; R, right; IPL, inferior parietal lobule.

ROI	Target cluster	MNI Coordinates			T value	Cluster size	Cluster-level uncorr p
		x	*y*	*z*			
R primary motor cortex	L V5	-44	-76	2	12.79	34	0.000101
R premotor cortex	L cerebellar crus I	-34	-70	-26	10.57	51	0.000002
L primary visual cortex	R inferior parietal lobule	44	-34	24	-10.38	25	0.000279

Table 5. MNI coordinates of clusters that showed post-bed rest FC changes that were significantly associated with changes in time to complete the Functional Mobility Test. Cluster size refers to the number of voxels in each cluster. Cluster-level uncorr p refers to uncorrected cluster size *p*-values. ROI, region of interest; L, left; R, right; uncorr, uncorrected.

Voxel-to-voxel analyses

Voxel-to-voxel brain-behavioral analyses did not yield any statistically significant clusters.

DISCUSSION

The aim of the current study was to investigate brain and behavioral effects of prolonged exposure to simulated microgravity and elevated CO_2 levels as a model of long-duration spaceflight onboard the International Space Station. To this end, we tested how 30 days of head-down tilt bed rest in 0.5% CO_2 affected resting-state functional brain connectivity. Our hypothesis-driven approach revealed that 30 days of HDBR in elevated CO_2 resulted in resting-state FC increases among vestibular, motor, and primary visual brain areas, which decreased following bed rest. These brain areas are involved in balance and spatial orientation, the planning, control, coordination and adaptation of voluntary movement, and low-level visual processing, respectively. In contrast, we found decreases in resting-state FC involving motor, somatosensory, vestibular, cognitive, and multimodal integration regions during bed rest, which increased following bed rest. These are brain areas implicated in voluntary movement planning, sensorimotor control and somatosensation, balance and spatial orientation, attention and awareness (Leech and Sharp, 2014), and visuospatial perception, respectively. Our hypothesis-free analysis revealed that connectivity within right primary visual cortex gradually decreased during the HDBR+CO_2 invention, then increased during the post-bed rest recovery phase. However, upon comparing the longitudinal ICC change of the HDBR+CO_2 group with those of the HDBR control group, the two groups did not show a significantly different pattern of ICC change -- although there was a trend toward greater decreases for the HDBR+CO_2 group.

Liao and colleagues (2012; 2013; 2015) have previously investigated resting-state activity changes during short duration HDBR interventions in ambient air. Employing a 7-day 6^o HDBR intervention, they examined changes in the amplitude of low frequency fluctuations (ALFF) at

baseline and on each day of their HDBR intervention. During bed rest, subjects exhibited increased ALFF in anterior cingulate cortex and the posterior lobe of the cerebellum as well as ALFF decreases in posterior cingulate cortex and left paracentral lobule (Liao et al., 2015). Here, we similarly found FC decreases involving posterior cingulate cortex during HDBR+CO_2. However, it is worth noting that Liao et al. (2015) did not leverage the longitudinal nature of their experimental design; they performed a one-way ANOVA across all time points followed by pairwise comparisons between each day of the HDT period versus the baseline phase.

Recent studies have examined the effects of long-duration HDBR in ambient air on large scale resting-state networks (Cassady et al., 2016; Zhou et al., 2014). Zhou et al (2014) used graph-theory based analyses to investigate pre- to post-bed rest FC changes. Following 45 days of HDBR in ambient air, subjects showed decreased degree centrality in the left anterior insula and dorsal anterior cingulate cortex. In the current study, we similarly observed widespread FC decreases involving insular cortices.

The current study built upon our recent work which demonstrated FC changes associated with 70 days of HDBR in ambient air. As in the current study, Cassady et al (2016) assessed connectivity changes from pre-, during, to post-bed rest using an analysis which incorporated both between- and within-subjects factors in the analysis. This type of analysis leveraged the longitudinal nature of the experimental design. It allowed for the identification of not only pre- to post-bed rest changes, but also the time course of FC changes throughout bed rest, using subjects' baseline measures as their own controls. Cassady et al (2016) showed gradual FC increases between primary motor and somatosensory cortices, and between vestibular cortex and lobule VI within the ipsilateral cerebellar hemisphere, which decreased after bed rest. They also showed gradual FC decreases between posterior parietal cortex and temporal-occipital cortex, between cerebellar lobule VIII and postcentral gyrus, and between the superior posterior fissure and crus I of the cerebellum. In the current study, we used similar analyses and identical regions of interests as Cassady et al (2016) to aid in drawing parallels between our results. Similar to the 70-day ambient air HDBR results, we observed gradual FC increases between vestibular cortex and the cerebellum with bed rest, albeit the cerebellar cluster here spanned Crus I and II of the contralateral hemisphere (which are part of the default mode network and networks involved in

cognitive control (Buckner et al., 2011). Reinforcing this similarity with the results of Cassady et al. (2016), the HDBR control group included in the present study exhibited a similar FC increase between vestibular cortex and crus I and II of the cerebellum as the HDBR+CO_2 group. This finding suggests that this result is driven by undergoing strict HDBR as opposed to the combination of HDBR and elevated CO_2. A notable qualitative difference between the results of the current study and those of Cassady et al (2016) is that HDBR+CO_2 resulted in a wider spread pattern of functional decoupling among motor, somatosensory, vestibular, cognitive, and multimodal integration brain areas.

To our knowledge, only one published study has examined resting-state FC changes following spaceflight. In their case study of a single cosmonaut who spent 169 days onboard the ISS, Demertzi et al (2016) reported post-flight reductions in intrinsic connectivity within the right insula and ventral posterior cingulate cortex as well as decreased FC between the cerebellum and motor cortex. It is noteworthy that the cosmonaut exhibited decreases in FC involving the insula and posterior cingulate cortex -- brain areas part of distributed networks that exhibited FC decreases during our HDBR+CO_2 intervention. Furthermore, we found that this functional encompassing bilateral insular cortices and right PCC exhibited a distinct pattern of FC changes during HDBR+CO_2 compared to our HDBR control group. This finding suggests that the observed connectivity changes were not due to strict HDBR alone, but rather were due to the combination of strict HDBR and elevated CO_2.

When comparing our results across resting-state fMRI studies of spaceflight and spaceflight analog environments, the most notable commonalities are FC decreases involving the insula and posterior cingulate cortex. The insula is an integral part of the vestibular network. The vestibular system uses multisensory cues (e.g., visual, somatosensory, auditory, and vestibular cues) for spatial orientation, self-motion perception, gaze stabilization, and postural control (Balaban, 2016). During spaceflight and in spaceflight analog environments, these multimodal cues provide incongruent information, requiring the central nervous system to adaptively reweight sensory inputs. The observed FC decreases among motor, somatosensory, vestibular, cognitive, and multimodal integration brain areas during HDBR+CO_2 may reflect such multisensory reweighting. The posterior cingulate cortex (PCC) is a core region of the default mode network,

817 which is activated during internally-focused cognition such as introspection, autobiographical
818 memory retrieval, etc. (Buckner et al., 2008). Regions within the PCC are also part of other
819 resting-state networks including the sensorimotor, salience, fronto-parietal, and dorsal attention
820 networks. The functional role(s) of the PCC remain debated, however, theories suggest its
821 involvement in internally-directed thought and controlling balance between external and internal
822 attention (Leech and Sharp, 2014). FC changes involving the PCC may be related to changes in
823 internally-focused cognition during bed rest. These commonalities support the validity of HDBR
824 as a model for studying spaceflight-associated functional neuroplasticity.
825
826 Moreover, unique to our HDBR+CO_2 intervention were FC changes involving visual brain areas,
827 namely primary visual cortex (V1) and lateral occipital cortex (LOC). V1 is involved in
828 processing low-level visual features (Tootell et al., 1998). LOC is involved in visual object
829 recognition, but is especially active when viewing inverted visual stimuli (e.g., faces and objects)
830 (Aguirre et al., 1999). This is an interesting finding since the subjects' heads were tilted down
831 and they would have had a partially inverted view of the experimenters and their surroundings.
832 Although a non-significant trend compared to our HDBR control group, our observation of
833 reduced ICC within V1 during HDBR+CO_2 is interesting in light of a recent 'multihit'
834 hypothesis that elevated CO_2 levels onboard the ISS contribute to the development of ophthalmic
835 abnormalities and visual impairments collectively known as Spaceflight Associated Neuro-
836 ocular Syndrome (SANS)(Zwart et al., 2017; Smith and Zwart, 2018), which affects
837 approximately 30% of astronauts returning from long-duration spaceflight (Mader et al., 2011;
838 Mader and Robert Gibson, 2017). This multihit hypothesis posits that a cascade of anatomical
839 and physiologic changes in microgravity (e.g., CO_2-induced cerebral blood flow increases,
840 headward fluid shifts, vascular leakage, edema) block CSF drainage which increases pressure on
841 the optic nerve and eye, ultimately resulting in neuro-ocular impairment (Zwart et al., 2017;
842 Smith and Zwart, 2018). It is feasible that increases in pressure exerted on the posterior segment
843 of the eye and/or the optic nerve could affect visual inputs to V1 and contribute to reduced
844 intrinsic connectivity. However, future study is needed to investigate this issue. Interestingly,
845 Laurie et al. (2019) collected optical coherence tomographic images before and at the end of
846 HDBR+CO_2. They found that 5 of the 11 subjects in the current study developed optic disc
847 edema -- one of the signs of SANS -- during the intervention. To our knowledge, this is the first

HDBR study to observe ophthalmic changes in participants. Comparisons of brain connectivity changes between the subgroups who did and did not develop signs of SANS during HDBR+CO_2 will be reported in a subsequent paper.

We also investigated if FC changes following HDBR+CO_2 were associated with behavioral performance alterations across subjects. We used a rod and frame test to estimate subjects' visual perception of true vertical. On average, subjects' responses became more consistent (i.e., lower response variability) during the HDBR+CO_2 intervention. This may reflect practice effects and/or the use of sensory reweighting as a strategy to improve trial-to-trial response consistency. We found that FC decreases between visual, vestibular and somatosensory brain areas were associated with increases in response consistency on the rod and frame test following bed rest. FC reductions between brain areas within the default mode network (i.e., PCC, SFG, and SPL (Buckner et al., 2008)) was also associated with improvements in response consistency. In contrast, subjects who exhibited increased FC between default mode network areas or between visual, vestibular and somatosensory brain areas tended to show increased response variability. The observed functional decoupling between visual, somatosensory and vestibular-related brain areas may reflect changes in sensory weighting that ultimately improve visual orientation perception following HDBR+CO_2.

Subjects exhibited varying degrees of slowing on the Functional Mobility Test following our HDBR+CO_2 intervention. FC increases between primary motor cortex (M1) and V5 (also known as hMT+, a higher order visual region involved in visual motion processing (Zeki et al., 1991)) and between premotor cortex and Crus I of the cerebellum were associated with greater slowing on the Functional Mobility Test after bed rest. Those subjects who exhibited decreases in FC between these areas showed less slowing. This finding suggests a link between functional decoupling among motor and higher order visual areas and less deterioration of locomotor abilities following HDBR+CO_2. We also found that FC decreases between V1 and inferior parietal lobule (IPL) were associated with greater slowing on the Functional Mobility Test. Subjects who exhibited FC increases between V1 and IPL showed less deterioration on the Functional Mobility Test. Primary visual cortex is involved in low-level visual processing (Tootell et al., 1998). It is believed that the IPL is involved in performing sensorimotor

879 transformations (Rushworth et al., 1998), with some studies also reporting its involvement
880 during preparation of foot movements (Sahyoun et al., 2004), and learning sequences of foot
881 movements (Lafleur et al., 2002). This result suggests a compensatory benefit of V1 and IPL
882 interactions following HDBR+CO_2.
883
884 Prolonged exposure to elevated CO_2 levels may affect brain vascular function and neural
885 activity, which cannot be disassociated using fMRI (Buxton, 2013). In the current study, Laurie
886 et al. (2019) acquired measures of end-tidal PCO_2, which did not show a significant change from
887 the beginning to the end of the HDBR+CO_2 intervention. Laurie et al. (2020) also recently
888 reported that arterial partial pressure of carbon dioxide ($PaCO_2$) and cerebrovascular reactivity to
889 CO_2 did not differ between the baseline and HDBR+CO_2 phases. However, analyses of blood
890 samples collected as part of NASA's standard measures assessment in the current study showed
891 a small but significant increase in $PaCO_2$ from pre- to post-HDBR+CO_2. Changes in cerebral
892 perfusion may therefore contribute to the observed brain connectivity changes. However, since
893 we did not have an ambulatory + CO_2 group, we cannot fully determine if any of the observed
894 brain changes are due to elevated CO_2 exposure alone.
895
896 A limitation of the current study is the small sample sizes for the HDBR+CO_2 (n=11) and HDBR
897 control (n=8) groups. While the inclusion of FC data from the HDBR control group provides
898 insight into whether the observed FC changes are due to strict HDBR or the combined effects of
899 CO_2 during strict HDBR, the HDBR control group is not ideal. First, the HDBR control data
900 were collected as part of a subsequent bed rest study which was conducted approximately one
901 year following data collection for the HDBR+CO_2 group. The timeline of the HDBR control
902 group differs from that of the HDBR+CO_2 group, with the HDBR control group undergoing 60
903 days of HDBR. The HDBR control group also included few females (6 males, 2 females).
904 Finally, practice effects on the rod and frame test performance present a further limitation.
905 Response variability on the rod and frame test showed a clear learning curve across sessions.
906 While post-bed rest increases in response variability support an effect of the HDBR+CO_2
907 intervention, it is currently not possible to disentangle effects of practice from the effects of the
908 HDBR+CO_2 intervention.
909

Here we investigated the time courses of resting-state FC changes from before, during, to after 30 days of HDBR in elevated CO_2. Our hypothesis-driven approach showed FC increases among visual, vestibular, and motor brain areas during HDBR+CO_2 which decreased following bed rest as well as widespread FC decreases among vestibular, visual, somatosensory and motor brain areas which increased following bed rest. Our hypothesis-free approach revealed a trend whereby FC decreases within primary visual cortex during HDBR+CO_2. We further examined relationships between FC changes and behavioral changes associated with HDBR+CO_2. We found that post-bed rest FC changes between visual, vestibular, and somatosensory regions were associated with changes in the consistency of visual perception of true vertical. Finally, we found that post-bed rest FC changes between visual and motor brain areas related to slowing of locomotor performance across subjects. We propose that these alterations of resting-state functional connectivity are a reflection of bed rest-associated multisensory reweighting and CO_2-related changes in cerebral perfusion. Our findings provide novel insight into the functional neuroplastic mechanisms underlying adaptation to HDBR+CO_2 microgravity analog environment. This knowledge will further improve HDBR as a model of microgravity exposure, and contribute to our knowledge of brain and performance changes during and after spaceflight.

REFERENCES

Aguirre, G.K., Singh, R., D'Esposito, M., 1999. Stimulus inversion and the responses of face and object-sensitive cortical areas. Neuroreport 10, 189–194.

Balaban, C.D., 2016. Neurotransmitters in the vestibular system. Handb. Clin. Neurol. 137, 41–55.

Behzadi, Y., Restom, K., Liau, J., Liu, T.T., 2007. A component based noise correction method (CompCor) for BOLD and perfusion based fMRI. Neuroimage 37, 90–101.

Benjamini, Y., Hochberg, H. (1995). Controlling the false discovery rate: a practical and powerful approach to multiple testing. *J. R. Stat. Soc. Seri B* 57, 289–300.

Biswal, B., Yetkin, F.Z., Haughton, V.M., Hyde, J.S., 1995. Functional connectivity in the motor cortex of resting human brain using echo-planar MRI. Magn. Reson. Med. 34, 537–541.

Bloomberg, J.J., Mulavara, A.P., 2003. Changes in walking strategies after spaceflight. IEEE Eng. Med. Biol. Mag. 22, 58–62.

Buckner, R.L., Andrews-Hanna, J.R., Schacter, D.L., 2008. The Brain's Default Network. Annals of the New York Academy of Sciences. https://doi.org/10.1196/annals.1440.011

Buckner, R.L., Krienen, F.M., Castellanos, A., Diaz, J.C., Yeo, B.T.T., 2011. The organization of the human cerebellum estimated by intrinsic functional connectivity. J. Neurophysiol. 106, 2322–2345.

Buxton, R. B. (2013). The physics of functional magnetic resonance imaging (fMRI). Reports on Progress in Physics, 76(9), 096601.

Carass, A., Cuzzocreo, J. L., Han, S., Hernandez-Castillo, C. R., Rasser, P. E., Ganz, M., ... & Thyreau, B. (2018). Comparing fully automated state-of-the-art cerebellum parcellation from magnetic resonance images. NeuroImage, 183, 150-172.

Cassady, K., Koppelmans, V., Reuter-Lorenz, P., De Dios, Y., Gadd, N., Wood, S., Castenada, R.R., Kofman, I., Bloomberg, J., Mulavara, A., Seidler, R., 2016. Effects of a spaceflight analog environment on brain connectivity and behavior. Neuroimage 141, 18–30.

Chumbley, J., Worsley, K., Flandin, G., & Friston, K. (2010). Topological FDR for neuroimaging. Neuroimage, 49, 3057–3064.

Cohen, H.S., Kimball, K.T., Mulavara, A.P., Bloomberg, J.J., Paloski, W.H., 2012. Posturography and locomotor tests of dynamic balance after long-duration spaceflight. J. Vestib. Res. 22, 191–196.

Cole, D.M., Smith, S.M., Beckmann, C.F., 2010. Advances and pitfalls in the analysis and interpretation of resting-state FMRI data. Front. Syst. Neurosci. 4, 8.

Courtine, G., Pozzo, T., 2004. Recovery of the locomotor function after prolonged microgravity exposure. I. Head-trunk movement and locomotor equilibrium during various tasks. Exp. Brain Res. 158, 86–99.

Damoiseaux, J.S., S A R, Barkhof, F., Scheltens, P., Stam, C.J., Smith, S.M., Beckmann, C.F., 2006. Consistent resting-state networks across healthy subjects. Proceedings of the National Academy of Sciences 103, 13848–13853.

Demertzi, A., Van Ombergen, A., Tomilovskaya, E., Jeurissen, B., Pechenkova, E., Di Perri, C., Litvinova, L., Amico, E., Rumshiskaya, A., Rukavishnikov, I., Sijbers, J., Sinitsyn, V., Kozlovskaya, I.B., Sunaert, S., Parizel, P.M., Van de Heyning, P.H., Laureys, S., Wuyts, F.L., 2016. Cortical reorganization in an astronaut's brain after long-duration spaceflight. Brain Struct. Funct. 221, 2873–2876.

Diedrichsen, J., 2006. A spatially unbiased atlas template of the human cerebellum. Neuroimage

33, 127–138.
Fox, M.D., Snyder, A.Z., Vincent, J.L., Corbetta, M., Van Essen, D.C., Raichle, M.E., 2005. The human brain is intrinsically organized into dynamic, anticorrelated functional networks. Proc. Natl. Acad. Sci. U. S. A. 102, 9673–9678.
Hargens, A.R., Vico, L., 2016. Long-duration bed rest as an analog to microgravity. J. Appl. Physiol. 120, 891–903.
Kanas, N., Manzey, D., 2008. Space Psychology and Psychiatry. https://doi.org/10.1007/978-1-4020-6770-9
Koppelmans, V., Bloomberg, J.J., De Dios, Y.E., Wood, S.J., Reuter-Lorenz, P.A., Kofman, I.S., Riascos, R., Mulavara, A.P., Seidler, R.D., 2017a. Brain plasticity and sensorimotor deterioration as a function of 70 days head down tilt bed rest. PLoS One 12, e0182236.
Koppelmans, V., Mulavara, A.P., Yuan, P., Cassady, K.E., Cooke, K.A., Wood, S.J., Reuter-Lorenz, P.A., De Dios, Y.E., Stepanyan, V., Szecsy, D.L., Gadd, N.E., Kofman, I., Scott, J.M., Downs, M.E., Bloomberg, J.J., Ploutz-Snyder, L., Seidler, R.D., 2015. Exercise as potential countermeasure for the effects of 70 days of bed rest on cognitive and sensorimotor performance. Front. Syst. Neurosci. 9, 121.
Koppelmans, V., Pasternak, O., Bloomberg, J.J., Dios, Y.E.D., Wood, S.J., Riascos, R., Reuter-Lorenz, P.A., Kofman, I.S., Mulavara, A.P., Seidler, R.D., 2017b. Intracranial Fluid Redistribution But No White Matter Microstructural Changes During a Spaceflight Analog. Sci. Rep. 7, 3154.
Lafleur, M.F., Jackson, P.L., Malouin, F., Richards, C.L., Evans, A.C., Doyon, J., 2002. Motor learning produces parallel dynamic functional changes during the execution and imagination of sequential foot movements. Neuroimage 16, 142–157.
Laurie, S. S., Macias, B. R., Dunn, J. T., Young, M., Stern, C., Lee, S. M. C., et al. 2019. Optic disc edema after 30 days of strict head-down tilt bed rest. Ophthalmology 126, 467–468.
Law, J., Van Baalen, M., Foy, M., Mason, S.S., Mendez, C., Wear, M.L., Meyers, V.E., Alexander, D., 2014. Relationship between carbon dioxide levels and reported headaches on the international space station. J. Occup. Environ. Med. 56, 477–483.
Laurie, S. S., Christian, K., Kysar, J., Lee, S. M., Lovering, A. T., Macias, B. R., ... & Stenger, M. B. (2020). Unchanged cerebrovascular CO2 reactivity and hypercapnic ventilatory response during strict head□down tilt bed rest in a mild hypercapnic environment. *J Physiol*.
Lee, J.K., De Dios, Y.E., Kofman, I.S., Mulavara, A.P., Bloomberg, J.J., Seidler, R.D. Head down tilt bed rest plus elevated CO2 as a spaceflight analog: Effects on cognitive and sensorimotor performance. Front. Human Neurosci., 13, 355.
Lee, J.K., Koppelmans, V., Riascos, R.F., Hasan, K.M., Pasternak, O., Mulavara, A.P., Bloomberg, J.J., Seidler, R.D., 2019. Spaceflight-Associated Brain White Matter Microstructural Changes and Intracranial Fluid Redistribution. JAMA Neurology. https://doi.org/10.1001/jamaneurol.2018.4882
Leech, R., Sharp, D.J., 2014. The role of the posterior cingulate cortex in cognition and disease. Brain. https://doi.org/10.1093/brain/awt162
Liao, Y., Lei, M., Huang, H., Wang, C., Duan, J., Li, H., Liu, X., 2015. The time course of altered brain activity during 7-day simulated microgravity. Front. Behav. Neurosci. 9, 124.
Liao, Y., Miao, D., Huan, Y., Yin, H., Xi, Y., Liu, X., 2013. Altered Regional Homogeneity with Short-term Simulated Microgravity and Its Relationship with Changed Performance in Mental Transformation. PLoS ONE. https://doi.org/10.1371/journal.pone.0064931

Liao, Y., Zhang, J., Huang, Z., Xi, Y., Zhang, Q., Zhu, T., Liu, X., 2012. Altered Baseline Brain Activity with 72 h of Simulated Microgravity – Initial Evidence from Resting-State fMRI. PLoS ONE. https://doi.org/10.1371/journal.pone.0052558

Lord, L.-D., Expert, P., Huckins, J.F., Turkheimer, F.E., 2013. Cerebral Energy Metabolism and the Brain's Functional Network Architecture: An Integrative Review. J Cerebral Blood Flow & Metab. https://doi.org/10.1038/jcbfm.2013.94

Mader, T.H., Gibson, C.R., Pass, A.F., Kramer, L.A., Lee, A.G., Fogarty, J., Tarver, W.J., Dervay, J.P., Hamilton, D.R., Sargsyan, A., Phillips, J.L., Tran, D., Lipsky, W., Choi, J., Stern, C., Kuyumjian, R., Polk, J.D., 2011. Optic disc edema, globe flattening, choroidal folds, and hyperopic shifts observed in astronauts after long-duration space flight. Ophthalmology 118, 2058–2069.

Mader, T.H., Robert Gibson, C., 2017. Early Evidence of Vision Impairment after Long-Duration Spaceflight. Intracranial Pressure and its Effect on Vision in Space and on Earth. https://doi.org/10.1142/9789814667111_0002

Manzey, D., Lorenz, B., 1998. Joint NASA-ESA-DARA Study. Part three: effects of chronically elevated CO2 on mental performance during 26 days of confinement. Aviat. Space Environ. Med. 69, 506–514.

Manzey, D., Lorenz, T.B., Heuers, H., Sangals, J., 2000. Impairments of manual tracking performance during spaceflight: more converging evidence from a 20-day space mission. Ergonomics 43, 589–609.

Martuzzi, R., Ramani, R., Qiu, M., Shen, X., Papademetris, X., Todd Constable, R., 2011. A whole-brain voxel based measure of intrinsic connectivity contrast reveals local changes in tissue connectivity with anesthetic without a priori assumptions on thresholds or regions of interest. NeuroImage. https://doi.org/10.1016/j.neuroimage.2011.06.075

McDonald, P.V., Basdogan, C., Bloomberg, J.J., Layne, C.S., 1996. Lower limb kinematics during treadmill walking after space flight: implications for gaze stabilization. Exp. Brain Res. 112, 325–334.

Miller, C.A., Peters, B.T., Brady, R.R., Richards, J.R., Ploutz-Snyder, R.J., Mulavara, A.P., Bloomberg, J.J., 2010. Changes in toe clearance during treadmill walking after long-duration spaceflight. Aviat. Space Environ. Med. 81, 919–928.

Moore, S.T., Dilda, V., Morris, T.R., Yungher, D.A., MacDougall, H.G., Wood, S.J., 2019. Long-duration spaceflight adversely affects post-landing operator proficiency. Sci. Rep. 9, 2677.

Mulavara, A.P., Feiveson, A.H., Fiedler, J., Cohen, H., Peters, B.T., Miller, C., Brady, R., Bloomberg, J.J., 2010. Locomotor function after long-duration space flight: effects and motor learning during recovery. Exp. Brain Res. 202, 649–659.

Mulavara, A.P., Peters, B.T., Miller, C.A., Kofman, I.S., Reschke, M.F., Taylor, L.C., Lawrence, E.L., Wood, S.J., Laurie, S.S., Lee, S.M.C., Buxton, R.E., May-Phillips, T.R., Stenger, M.B., Ploutz-Snyder, L.L., Ryder, J.W., Feiveson, A.H., Bloomberg, J.J., 2018. Physiological and Functional Alterations after Spaceflight and Bed Rest. Med. Sci. Sports Exerc. 50, 1961–1980.

Paloski, W.H., Bloomberg, J.J., Reschke, M.F., Harm, D.L., 1994. Spaceflight-induced changes in posture and locomotion. J Biomech. https://doi.org/10.1016/0021-9290(94)91366-8

Paloski, W.H., Reschke, M.F., Black, F.O., Doxey, D.D., Harm, D.L., 1992. Recovery of postural equilibrium control following spaceflight. Ann. N. Y. Acad. Sci. 656, 747–754.

Pavy-Le Traon, A., Heer, M., Narici, M.V., Rittweger, J., Vernikos, J., 2007. From space to

Earth: advances in human physiology from 20 years of bed rest studies (1986-2006). Eur. J. Appl. Physiol. 101, 143–194.

Poldrack RA, Mumford JA. Independence in ROI analysis: where is the voodoo? Soc Cogn Affect Neurosci 4: 208 –213, 2009.

Raichle, M.E., 2010a. Two views of brain function. Trends in Cog. Sci. https://doi.org/10.1016/j.tics.2010.01.008

Raichle, M.E., 2010b. The Brain's Dark Energy. Scientific American. https://doi.org/10.1038/scientificamerican0310-44

Reschke, M.F., Bloomberg, J.J., Harm, D.L., Paloski, W.H., Layne, C., McDonald, V., 1998. Posture, locomotion, spatial orientation, and motion sickness as a function of space flight. Brain Res. Brain Res. Rev. 28, 102–117.

Reschke, M.F., Bloomberg, J.J., Paloski, W.H., Mulavara, A.P., Feiveson, A.H., Harm, D.L., 2009. Postural reflexes, balance control, and functional mobility with long-duration head-down bed rest. Aviat. Space Environ. Med. 80, A45–54.

Roberts, D.R., Albrecht, M.H., Collins, H.R., Asemani, D., Rano Chatterjee, A., Vittoria Spampinato, M., Zhu, X., Chimowitz, M.I., Antonucci, M.U., 2017. Effects of Spaceflight on Astronaut Brain Structure as Indicated on MRI. New Eng J Med. https://doi.org/10.1056/nejmoa1705129

Romero, J.E., Coupé, P., Giraud, R., Ta, V.-T., Fonov, V., Park, M.T.M., Mallar Chakravarty, M., Voineskos, A.N., Manjón, J.V., 2017. CERES: A new cerebellum lobule segmentation method. NeuroImage. https://doi.org/10.1016/j.neuroimage.2016.11.003

Rushworth, M.F., Johansen-Berg, H., Young, S.A., 1998. Parietal cortex and spatial-postural transformation during arm movements. J. Neurophysiol. 79, 478–482.

Sahyoun, C., Floyer-Lea, A., Johansen-Berg, H., Matthews, P.M., 2004. Towards an understanding of gait control: brain activation during the anticipation, preparation and execution of foot movements. Neuroimage 21, 568–575.

Schulte, J.H., 1964. Sealed environments in relation to health and disease. Arch. Environ. Health 8:438-452.

Smith, S.M., Zwart, S.R., 2018. Spaceflight-related ocular changes: the potential role of genetics, and the potential of B vitamins as a countermeasure. Curr. Opin. Clin. Nutr. Metab. Care 21, 481–488.

Tootell, R.B.H., Hadjikhani, N.K., Vanduffel, W., Liu, A.K., Mendola, J.D., Sereno, M.I., Dale, A.M., 1998. Functional analysis of primary visual cortex (V1) in humans. Proc. Nat. Acad. Sci. https://doi.org/10.1073/pnas.95.3.811

Van Dijk, K.R.A., Sabuncu, M.R., Buckner, R.L., 2012. The influence of head motion on intrinsic functional connectivity MRI. NeuroImage. https://doi.org/10.1016/j.neuroimage.2011.07.044

Welch, R.B., Hoover, M., Southward, E.F., 2009. Cognitive performance during prismatic displacement as a partial analogue of "space fog." Aviat. Space Environ. Med. 80, 771–780.

Whitfield-Gabrieli, S., Nieto-Castanon, A., 2012. Conn: A Functional Connectivity Toolbox for Correlated and Anticorrelated Brain Networks. Brain Connect. 2, 125–141.

Yuan, P., Koppelmans, V., Reuter-Lorenz, P.A., De Dios, Y.E., Gadd, N.E., Wood, S.J., Riascos, R., Kofman, I.S., Bloomberg, J.J., Mulavara, A.P., Seidler, R.D., 2016. Increased Brain Activation for Dual Tasking with 70-Days Head-Down Bed Rest. Front. Syst. Neurosci. 10, 71.

Yuan, P., Koppelmans, V., Reuter-Lorenz, P., De Dios, Y., Gadd, N., Riascos, R., Kofman, I.,

Bloomberg, J., Mulavara, A., Seidler, R.D., 2018a. Change of cortical foot activation following 70 days of head-down bed rest. J. Neurophysiol. 119, 2145–2152.

Yuan, P., Koppelmans, V., Reuter-Lorenz, P., De Dios, Y., Gadd, N., Wood, S., Riascos, R., Kofman, I., Bloomberg, J., Mulavara, A., Seidler, R., 2018b. Vestibular brain changes within 70 days of head down bed rest. Hum. Brain Mapp. 39, 2753–2763.

Zeki, S., Watson, J.D., Lueck, C.J., Friston, K.J., Kennard, C., Frackowiak, R.S., 1991. A direct demonstration of functional specialization in human visual cortex. J. Neurosci. 11, 641–649.

Zeng, L.-L., Liao, Y., Shen, H., Liu, X., Hu, D., 2016. Decoding Brain States with Simulated Microgravity from Baseline Using Functional Connectivity of Default Network. Adv. Cogn Neurodyn. (V). https://doi.org/10.1007/978-981-10-0207-6_45

Zhou, Y., Wang, Y., Rao, L.-L., Liang, Z.-Y., Chen, X.-P., Zheng, D., Tan, C., Tian, Z.-Q., Wang, C.-H., Bai, Y.-Q., Chen, S.-G., Li, S., 2014. Disrupted resting-state functional architecture of the brain after 45-day simulated microgravity. Front. Behav Neurosci. https://doi.org/10.3389/fnbeh.2014.00200

Zwart, S.R., Gibson, C.R., Gregory, J.F., Mader, T.H., Stover, P.J., Zeisel, S.H., Smith, S.M., 2017. Astronaut ophthalmic syndrome. FASEB J. 31, 3746–3756.